Accepted Manuscript


# ZEP520A — A resist for electron-beam grayscale lithography and thermal reflow

R. Kirchner, V.A. Guzenko, I. Vartiainen, N. Chidambaram, H. Schift

PII: S0167-9317(16)30017-X
DOI: doi: 10.1016/j.mee.2016.01.017
Reference: MEE 10087

To appear in:

Received date: 7 November 2015
Revised date: 13 January 2016
Accepted date: 19 January 2016

Please cite this article as: R. Kirchner, V.A. Guzenko, I. Vartiainen, N. Chidambaram, H. Schift, ZEP520A — A resist for electron-beam grayscale lithography and thermal reflow, (2016), doi: 10.1016/j.mee.2016.01.017

This is a PDF file of an unedited manuscript that has been accepted for publication. As a service to our customers we are providing this early version of the manuscript. The manuscript will undergo copyediting, typesetting, and review of the resulting proof before it is published in its final form. Please note that during the production process errors may be discovered which could affect the content, and all legal disclaimers that apply to the journal pertain.

ACCEPTED MANUSCRIPT

# ZEP520A - a resist for electron-beam grayscale lithography and thermal reflow

R. Kirchner[a], V. A. Guzenko[a], I. Vartiainen[a,b], N. Chidambaram[a], H. Schift[a]

[a] *Paul Scherrer Institut, Laboratory for Micro- and Nanotechnology, 5232 Villigen PSI, Switzerland*
[b] *University of Eastern Finland, Institute of Photonics, 80101 Joensuu, Finland*

**Abstract**

The usability of ZEP520A as resist for thermally activated selective topography equilibration (TASTE) was investigated. It was found that (i) a high-contrast resist such as ZEP520A is well suitable for grayscale electron-beam lithography, (ii) a selective thermal reflow is possible with ZEP520A and (iii) reflow is governed by the same energy minimization principle as known from poly (methyl methacrylate) (PMMA), another linear thermoplastic resist. The high contrast of ZEP520A does not play a role for the step-to-step sidewall angle as this is only governed by the design of the step. ZEP520A and similar positive tone resists on the market provide the same reflow-feature variety as PMMA including stable and unstable, concave and convex, arbitrary stepped and sloped features as well as combinations of all these features. The advantage of ZEP520A is a reduced writing time due to its high sensitivity. Finally, the transfer of the reflow process to structures being much smaller than typical TASTE structures so far was demonstrated.

*Keywords:* sensitivity, contrast, sidewall inclination, energy optimization, thermoplastic, visco-elasticity, polymer

## 1. Introduction

Improving the performance of microelectronics was for a very long time enabled by shrinking the size of functional units and, thus, by increasing their areal density. Since some time, performance improvement comes mainly from functional improvement and new architectures like multi-cores or Fin-FETs and vertical memory stacking [1, 2]. Fin-FETs and vertical memories already use an out-of-plane, or 3D, patterning and integration. Emerging high-end, high-volume applications and heterogeneous system integration will require more and advanced 3D lithography and replication techniques [3]. Such advanced methods are for example top-down grayscale and 3D lithography based on electrons [4–6], ions [7], photons [8] or full-3D methods such as 2-photon-lithography [9–11] or other methods based on sophisticated material control [12–16].

This paper discusses the use of high-sensitivity and high-contrast electron-beam resists for high-resolution, out-of-plane, grayscale electron-beam lithography (EBL). In contrast, the working horse of grayscale EBL so far were low-contrast, positive resists such as poly (methyl methacrylate) (PMMA), a well established electron-beam and nanoimprint lithography resist. Polymer reflow is known as fabrication technique for microlenses [17–20]. Recently, a thermal reflow technique termed temperature activated selective topography equilibration (TASTE), exploiting the thermoplastic behavior of grayscale electron beam exposed PMMA, was introduced to make ultra-smooth concave, convex or combined structures [21]. PMMA with suited molecular weight, such as the PMMA120k reference material of this study, was proofed to be even useful for a combined nanoimprint and grayscale electron beam lithography [22]. The resist tested in this work, ZEP520A, is also a linear, thermoplastic polymer like PMMA. Thus, thermoplastic reflow and a principle usability for TASTE was expected from ZEP520A. ZEP has further some substantial advantages over PMMA: The high refractive index of about 1.56 ($\lambda$=589 nm) [23] allows to reach improved light confinement compared to PMMA with a typical refractive index of only about 1.49 ($\lambda$=589 nm). The higher sensitivity enables, depending on the selected development regime, more than two times faster writing. The higher etch selectivity allows for a better pattern transfer into the substrate. Interesting work is ongoing to develop competitive and partly similar resists to PMMA and ZEP520A. Competitive materials for those two workhorse-resist are for example GL2000 [24], CSAR62 [25, 26] or

*Email addresses:* robert.kirchner@psi.ch (R. Kirchner), helmut.schift@psi.ch (H. Schift)

ACCEPTED MANUSCRIPT

Figure 1: Schematic overview on sample preparation and evaluation: a) dose-modulated electron-beam grayscale patterning with different doses between $D_{100} = 0\,\mu C/cm^2$ (full resist height) )and $D_0$ (dose-to-clear), b) resulting different heights within the same wet development step due to different doses, c) different reflow behavior depending on the exposure dose and thus the resulting molecular weight $M_w$ and $T_g$ and d) evaluation of the reflow behavior based on the apparent contact angle $\Theta$ between resist and substrate that was observed for different reflow times.

mr-PosEBR [27], a recent development under commercialization, having all a closely related chemical formulation to ZEP520A and partly similar properties. There is furthermore SML [28, 29] with etch properties close to ZEP520A and a sensitivity close to PMMA. The grayscale patterning and reflow performance of ZEP520A was tested as a representative example for these resists. Two issues were investigated: (i) the effect of the development anisotropy due to differences in contrast on the grayscale pattern sidewall inclinations and (ii) the reflow behavior upon thermal activation due to a pronounced reduction of the glass transition temperature during exposure.

## 2. Experimental

### 2.1. Grayscale patterning

ZEP520A is a copolymer of $\alpha$-methylstyrene and $\alpha$-chloromethacrylate. The high electron absorption due to chlorine is the main origin of its high sensitivity [30]. The methylstyrene accounts for a higher dry etch resistance compared to PMMA. It was assumed, that the electron-beam patterning of ZEP520A is based on molecular chain scission similar to PMMA [27, 31]. Electron-beam grayscale patterning was achieved with a 100 kV system (EBPG 5000 Plus, Vistec Lithography B.V.) on a 558 nm thick ZEP520A (ZEON Corp.) resist film. The resist was spun on an oxygen plasma cleaned and annealed (250°C, 5 min) silicon substrate. Solvent was removed after spin-coating by annealing for 3 min at 180°C. Reference samples were prepared from anisole diluted PMMA120k (micro resist technology GmbH) with a thickness of 475 nm on identical substrates. Anisole was removed on a hotplate at 140°C for 2 min. Dose patterns of 100 µm wide squares were used to determine the contrast curve. With a contrast-curve-based approach, different doses were then applied to get the desired structure height (e.g. $D_{50}$ to get 50% of the resist height) (Fig. 1a). The higher the EBL dose, the lower is the molecular weight $M_w$ due to chain scission [21, 31]. Consequently, the solubility, and thus the development rate in a given developer is higher for larger doses (Fig. 1b). The development was done in ethyl-3-ethoxypropionate (EEP), methyl isobutyl ketone (MIBK) and the commercial developer ZED-N50 for the ZEP520A. For the PMMA 120k also MIBK, EEP and a mixture of isopropyl alcohol (IPA) with MIBK (MIBK:IPA 1:3) were used. ZEP520A and PMMA samples were rinsed in DI-water to stop the development and finally blown dry by nitrogen. Crystal-orientation based substrate cleaving and scanning electron microscopy (SEM) cross section inspection of as-developed samples were used to experimentally determine the sidewall angles of the grayscale patterns.

Figure 2: Contrast curves of ZEP520A and PMMA120k for different resist-developer systems that are used for grayscale electron-beam lithography. The curves were obtained by temperature controlled development of micron-sized test patterns.

### 2.2. Thermal reflow

The higher the EBL dose is, the lower is the glass transition temperature $T_g$ [21] and the faster the reflow [32, 33]. Thermal reflow was performed on a temperature controlled hotplate for different periods of time (Fig. 1c). After reflow, the samples were immediately cooled down to room temperature to "freeze" the reflowed shape for further inspection. Again, SEM cross-section inspection of cleaved structures was used to get the reflowed profile. For this, about 100 µm extended patterns of single lines, double-steps and multi-steps were tested. Finally, the apparent contact angle (Fig. 1d and e.g. Fig. 6) as well as the polymer surface structure of the cleaving facets were used to investigate the reflow behavior. The resist reflow is a creep-like material displacement along the substrate being driven by wetting forces and being governed by the involved surface free energies and the mobility (viscosity) of the polymer [32, 33].

## 3. Results and discussion

This sections discusses the experimentally found contrast behavior for PMMA120k and ZEP520A, gives the developed theoretical model for the sidewall inclination and finally evaluates this model against experimental measurements using two selected resist-developer systems.

### 3.1. Experimental contrast evaluation

Depending on the used developer, with ZEP520A one can achieve much higher contrast than using PMMA

ACCEPTED MANUSCRIPT

Table 1: Contrast $\gamma$ for different developer-resist systems at 20°C being obtained using piecewise linear fits. The contrast range is given by a piecewise linear fit using either two- or three-segments. The three-segment fit matches well the standard definition in Eq. (1), but the two-segment fit considers better the top loss in more aggressive developers.

| Developer / Resist | PMMA120k | ZEP520A |
|---|---|---|
| | range: 2-3 segment fit | |
| MIBK | 2.5-2.8 | 6.2-6.2 |
| MIBK:IPA 1:3 | 3.6-4.2 | - |
| EEP | 2.8-3.2 | 2.9-3.5 |
| N50 | - | 6.5-6.5 |

(Fig. 2). From the contrast curves, the contrast $\gamma$ was determined based on the standard definition

$$\gamma = log_{10}\,(D_{100*}/D_0)^{-1} \qquad (1)$$

using piecewise linear fits with two and three linear segments which approximated the contrast curves very well (Tab. 1). $D_0$ represents the dose-to-clear value. $D_{100*}$ is the value extrapolated for the intersection of the piecewise linear fit going through $D_0$ and the horizontal line at a relative height of 1.0 in Fig. 2. The most sensitive resist-developer system ZEP520A-EEP was used for grayscale and reflow experiments as it best minimized the writing time within this study.

### *3.2. Theoretical model for the sidewall inclination*

The dose determines the amount of material that is removed in a given time, or in other words the development rate $r$, in the respective area. As will be shown, the step-to-step sidewall inclination depends on these development rates of the adjacent regions (Fig. 3). Wet development is basically an isotropic etching process. The lateral development rate of the sidewall of a certain step is the same as the vertical development rate of this step. This means while the step height is reduced with increasing development time, the width of this step is also reduced at the same time. The top of the step is exposed longer to the developer than the footing area. This leads to a tapering or an inclined step-to-step sidewall with a certain angle. This angle $\alpha$ can be determined from

$$\alpha = 90° - arcsin\,(r_1/r_2) \qquad (2)$$

where $r_1$ and $r_2$ are the dose-dependent development rates of the respective steps 1 and 2 [34]. This model is based on the following considerations in Fig. 3: The development rate of step 2 is higher than that of step 1 and a convex corner is formed between step 1 and step 2. In an idealistic scenario (Fig. 3a), the two steps behave independent of each other. Each development front moves at different rates defining a certain step configuration after a certain time. However, in the realistic scenario (Fig. 3b), the convex corner undergoes lateral development. This lateral development depends on the development rate of step 1. Eq. (2) can be obtained from trigonometric considerations in Fig. 3b. As a consequence, a high contrast resist does not improve the angle $\alpha$ between differently exposed and adjacent steps. This angle is independent of the resist contrast, it depends only on contrast-independent development rates. It can be also intuitively understood by the fact that a 50% resist removal always requires a development rate that is half that of a 100% resist removal. The required development rate ratio is the same for different resists. Only the angle between unexposed and exposed regions can be influenced by the resist-developer system. This is due to the dependence of the development rate in the unexposed region, the so-called top loss, on the resist-developer system.

Figure 3: Theoretical model for the evolution of the step-to-step sidewall angles using discrete points in time from $t_0$ to $t_3$ where $t_0$ is the starting point of the development: The angles are solely depending on the development rates ($r_2 > r_1$) of the respective steps being exposed with different doses ($D_2 > D_1$). The a) ideal development case does not consider lateral development, while b) in the real experimental development situation lateral development is significant.

Figure 4 shows the theoretically achievable angles $\alpha$ for a multi-step pattern of five levels as depicted in the inset. The theoretical curve (solid line) is calculated from Eq. (2). Additionally, angles $\alpha$ calculated from experimentally measured development rates (cf. Fig. 2) being required for the respective five-level configuration are overlaid. The sidewall angles decrease with decreasing step height. As expected, $\alpha_3$ through $\alpha_5$ coincide with each other, even though the contrast curves, and thus, the development rates are completely different (cf. Fig. 2). This confirms that the sidewall angle is independent of the contrast. The co-development of each step will unavoidable lead to an independence between the step-to-step angles and the resist-developer contrast. Angles $\alpha_1$ and $\alpha_2$ scatter along the theoretical plot and do not coincide for different resist-developer systems. This is because the development rate of the involved unexposed step is given by the top loss, which is dependent on the resist-developer system as discussed before. As in binary lithography, minimizing this loss is the only improvement one can obtain by using a high contrast system for grayscale lithography. For example the low-contrast developer EEP or MIBK have a signif-

ACCEPTED MANUSCRIPT

Figure 4: Plot of the sidewall angle versus the ratio of the development rates obtained from Eq. (2) together with theoretical sidewall angles expected from experimentally measured development rates from different resist-developer contrast curves. The sidewall angles $\alpha$ are defined in Fig. 3 and the order is always from $\alpha_1$ through $\alpha_5$ with decreasing sidewall angle values.

Figure 5: Theoretical plot from Fig. 4 overlaid with real angle values obtained from SEM cross-sections including a large variety of step designs. The error bars give the standard deviation for the respective mean data points.

icant top loss for ZEP520A and PMMA (cf. Fig. 2, rel. thickness 0.95-1.00), respectively. This leads to reduced $\alpha_1$- and $\alpha_2$-values for ZEP520A-EEP, and even more for PMMA120k-MIBK, compared to the high-contrast system ZEP50A-N50. Please note, the top loss of the unexposed section partly depends on the structure size due to the proximity effect being the main origin for this loss. The proximity effect is a crosstalk effect and is caused by scattered electrons increasing the affected area beyond the really exposed area. For this reason, unexposed areas also receive a certain dose. Depending on the contrast curve this leads to an unwanted development, or top-loss, in these areas. The effect decreases with distance from the exposed area.

### *3.3. Experimental evaluation of the theoretical model*

Figure 5 compares the theoretical curve (solid line) with experimental step-to-step sidewall angles (empty data points) from cross sections (e.g. Fig. 6i). The data is based on a subset of three experiments including 112 individual SEM measurements. The theoretical values are based on Eq. (2). The experimental points were obtained from SEM height measurements. The rate ratio was calculated from the ratio of removed resist, which gives by definition the same value. The related angles are obtained from the same SEM cross-sections. The experimental measurements follow the theoretically expected behavior and the sidewall angle decreases towards lower steps. This is a consequence of the co-development of the steps as already discussed in the theoretical model above. Which is, as discussed before, the inherent consequence of the co-development process and was observed in all experiments. However, there was a considerable variation which probably originated from experimental deviations. Especially $\alpha_5$ is more sensitive to errors because the data point position depends on the accurate stopping of the development process as soon as the substrate is cleared.

### *3.4. Reflow shapes using ZEP520A*

It was assumed that upon exposure with electrons, the molecular weight of ZEP520A is reduced similar to PMMA. This was empirically confirmed by the appearance of the granular structure after cleaving in exposed and unexposed sections (cf. Fig. 6g,i). A larger dose results in a smaller $M_w$ and granularity. The original molecular weight of unexposed ZEP520A is $M_w = 57 kg/mol$ [23]. The $T_g$ of ZEP520A was measured by differential scanning calorimetry (DSC, DSC Q1000, TA Instruments) to be about 121-122°C. The heating rate was $10\,K/min$. For the measurement, the cast resist was "harvested" from clean glass samples after 1.5h annealing at the recommended temperature of 180°C. The resist provider gives a $T_g$ value of about 105°C [23]. However, experimental results of this study (cf. Sec. 3.5 and Ref. [32]) confirmed a higher $T_g$. This is also in agreement with the onset of reflow of thin films at about 145°C [35]. The reflow at 145°C enabled sufficient structural contrast: As visible in Figure 6a,b, unexposed shapes do deform to a minor extent only, while exposed steps such as in Figure 6e,f show a significant reflow towards constant curvature shapes. This is expected from an energy-optimizing process like reflow. The clear deformation of the unexposed line in Figure 6c,d originates from the relative contribution of the moving material in relation to the overall structure. For example in Fig. 6a,b the width increase after reflow is about 10% and thus small compared to the original structure width. Therefore, the overall shape does not change significantly. However, in Fig. 6c,d the width increase is about 90%. This is a significant relative amount and the overall shape has to change a lot. To keep the cross-section area constant (volume conservation), the height has to be reduced significantly in Fig. 6c,d while the height in Fig. 6a,b stays more or less constant. The combination of unexposed and exposed steps demonstrate the ability for a selective reflow of only the exposed sections (Fig. 6g,h). This is the typical behavior published before for PMMA [32] which depends on different resist molecule mobilities (viscosities) [33]. With multiple steps other slopes and even concave shapes can be obtained depending on the initial step-geometry (Fig. 6i,j). This demonstrates the full useability of ZEP520A for grayscale patterning and TASTE. The writing time for the same patterns were about half the time for ZEP520A compared to PMMA120k. This can be already anticipated from the contrast curve (cf. Fig.2) with ZEP520A having half the required doe-to-clear compared to PMMA120k.

ACCEPTED MANUSCRIPT

Figure 6: SEM cross-sections of long extended lines compared before and after reflow: minor structural effect for the reflow of a) a single unexposed line giving b) a stable line, large effect for c) a small unexposed but high aspect-ratio line giving d) a collapsed line, reflow leading to transformation of e) a single exposed line (79 $\mu C/cm^2$) into f) an almost constant curvature cylindrical lens, transformation of g) a double step with unexposed and exposed (99 $\mu C/cm^2$) section into h) an asymmetric structure with a slope of about 43° and one of about 69°, transformation of i) a multi-step structure having of one unexposed and three exposed (79, 99 and 111 $\mu C/cm^2$) steps into j) an asymmetric feature with a concave formed section and one steep 69° section. (All scale bars: 200 nm)

### *3.5. Time dependent reflow of ZEP520A*

For the unexposed material an extremely slow movement along the substrate, expressed as slowly decreasing apparent contact angle, was observed (Fig. 7,8). In contrast, the higher doses showed a clear and fast exponential decay of the apparent contact angle as observed before for PMMA [32]. The decay approached an asymptotic limit. This limit depends on the molecular weight and thus on the exposure dose. However, this effect is not as pronounced as for PMMA120k ($M_w = 92kg/mol$) [32]. This might be based on the lower initial $M_w$ of ZEP520A and thus the lower $M_w$- and $T_g$-contrast that is especially expected for higher doses.

The structure size also defines the reflow behavior (Fig. 7 vs. 8). It is important to note that the initial apparent contact angles for small and wide lines are comparable. Smaller structures reflow faster than bigger ones and tend to have slightly smaller asymptotic limits. This is also in agreement with previous observations [32]. It might be caused by some proximity exposure effects that reduce the molecular weight of the resist line especially at the periphery. However, more probable is the relative contribution of the material that is moving. This is the relation of the width change in respect to the total cross-sectional area of the reflowing structure as discussed before (cf. Sec. 3.4).

The results with ZEP520A point again to the fact that a reflow close to the glass transition is not just a viscous flow. It is a visco-elastic behavior and the final shape is not only governed by the reflow time. Different final apparent contact angles for different molecular weights clearly demonstrate that forces must exist that limit the reflow, or better creep, of the polymer along the substrate. Possible forces are restorative, or counteracting, forces acting on the polymer chains and limiting their ability to move. The reflowed structure should finally be under tensile stress. The polymer chains cannot freely flow but are rather acting like extended springs in an entangled network. Depending on the molecular weight, the spring constant is different. However, the pulling force by wetting is constant. This gives differently extended springs for different molecular weights. Below a certain molecular weight, no entanglements exist and the material flow is viscous and the polymer feature can obtain its energetically optimal shape.

Figure 7: Behavior of the apparent contact angle between an about 250 nm wide reflowing resist line and the silicon substrate over time.

Figure 8: Behavior of the apparent contact angle between an about 500 nm wide reflowing resist line and the silicon substrate over time.

## 4. Conclusions

ZEP520A has a comparable grayscale patterning performance and is a viable alternative for PMMA in the TASTE process. The findings of this paper together with previous results clearly demonstrate that selective reflow, observed for PMMA and ZEP, is of general nature: A temperature selective reflow can be achieved by different materials and radiation based methods providing a sufficient contrast in molecular weight, and thus, $T_g$. Reflow is a surface-tension driven, visco-elastic creep process limited by molecular mobility of polymer chains.

As demonstrated, the contrast of the developer-resist system does not influence the step-to-step sidewall angle except the steps involving unexposed resist. A higher contrast requires a more accurate dose control. As the higher contrast gives no benefit, medium- or even low-contrast resist-developer systems can be used to achieve a much better process control and step-height precision. The benefit of ZEP520A and similar resists is the higher sensitivity and therewith the faster patterning.

## Acknowledgment

The authors express their special thanks to A. Pascual (University of Applied Sciences and Arts Northwestern Switzerland) for the DSC measurements.

## References

[1] A. D. Franklin, Science 349 (2015) aab2750 (10 pp).
[2] J. Kim, A. J. Hong, S. M. Kim, K. Shin, E. B. Song, Y. Hwang, F. Xiu, K. Galatsis, C. O. Chui, R. N. Candler, S. Choi, J.-T. Moon, K. L. Wang, Nanotechnology 22 (2011) 254006 (7pp).
[3] R. Kirchner, H.Schift, Microelectron. Eng. 141 (2015) 243–244.
[4] Y. Hirai, S. Harada, H. Kikuta, Y. Tanaka, M. Okano, S. Isaka, M. Kobayasi, J. Vac. Sci. Technol. B 20 (2002) 2867–2871.
[5] F. Hu, S.-Y. Lee, J. Vac. Sci. Technol. B 21 (2003) 2672–2679.

ACCEPTED MANUSCRIPT


[6] Y. Shinonaga, K. Ogino, N. Unno, S. Yoshida, M. Yamamoto, J. Taniguchi, Microelectron. Eng. 141 (2015) 102–106.

[7] K. Keskinbora, C. Grévent, M. Hirscher, M. Weigand, G. Schütz, Adv. Opt. Mater. 3 (2015) 792–800.

[8] H. Sato, H. Matsumura, S. Keino, S. Shoji, J. Micromech. Microeng. 16 (2006) 2318–2322.

[9] S. Maruo, J. T. Fourkas, Laser Photon. Rev. 2 (2008) 100–111.

[10] J. Fischer, M. Wegener, Laser Photon. Rev. 7 (2013) 22–44.

[11] C. Donnelly, M. Guizar-Sicairos, V. Scagnoli, M. Holler, T. Huthwelker, A. Menzel, I. Vartiainen, E. Müller, E. Kirk, S. Gliga, J. Raabe, L. J. Heyderman, Phys. Rev. Lett. 114 (2015) 115501.

[12] D. H. Gracias, V. Kavthekar, J. C. Love, K. E. Paul, G. M. Whitesides, Adv. Mater. 14 (2002) 235–238.

[13] J.-H. Cho, M. D. Keung, N. Verellen, L. Lagae, V. V. Moshchalkov, P. V. Dorpe, D. H. Gracias, small 7 (2011) 1943–1948.

[14] J. J. Balowski, Y. Wang, N. L. Allbritton, Adv. Mater. 25 (2013) 4107–4112.

[15] C. A. Ross, K. K. Berggren, J. Y. Cheng, Y. S. Jung, J.-B. Chang, Adv. Mater. 26 (2014) 4386–4396.

[16] C. Chen, Z. Xie, X. Wei, Z. Zheng, Small 11 (2015) 6013–6017.

[17] Y. Ishihara, K. Tanigaki, in: Proc. Int. Electron Devices Meeting, volume 29, pp. 497–500.

[18] Z. D. Popovic, R. A. Sprague, G. A. N. Connell, Appl. Optics 27 (1988) 1281–1284.

[19] F. T. O'Neill, J. T. Sheridan, Optik 113 (2002) 391–404.

[20] S. Audran, B. Mortini, B. Faure, G. Schlatter, J. Micromech. Microeng. 20 (2010) 095008 (9pp).

[21] A. Schleunitz, V. Guzenko, M. Messerschmidt, H. Atasoy, R. Kirchner, H. Schift, Nano Converg. 1:7 (2014) 1–8.

[22] A. Schleunitz, C. Spreu, M. Vogler, H. Atasoy, H. Schift, J. Vac. Sci. Technol. B 29 (2011) 06FC01 (4pp).

[23] ZEON CORPORATION - Electronics Materials Division, ZEP520A, Technical Report, Ver.2 Oct.2010, 2012.

[24] M. Otani, H. Asada, H. Tsunoda, M. Kunitake, T. Ishizaki, R. Miyagawa, Proc. SPIE 8081 (2011) 808107 (8 pp).

[25] M. Schirmer, B. Büttner, F. Syrowatka, G. Schmidt, T. Köpnick, C. Kaiser, Proc. SPIE 8886 (2013) 88860D (7pp).

[26] S. Thoms, D. S. Macintyre, J. Vac. Sci. Technol. B 32 (2014) 06FJ01 (7pp).

[27] S. Pfirrmann, O. Lohse, V. Guzenko, A. Voigt, I. Harder, A. Kolander, G. Grützner, Microelectron. Eng. - (2015) –. [submitted to Special Issue MNE 2015].

[28] M. A. Mohammad, S. K. Dew, M. Stepanova, Nanoscale Research Letters 8:139 (2013) 7pp.

[29] A. Gangnaik, Y. M. Georgiev, B. McCarthy, N. Petkov, V. Djara, J. D. Holmes, Microelectron. Eng. 123 (2014) 126–130.

[30] M. A. Mohammad, K. Koshelev, T. Fito, D. A. Z. Zheng, M. Stepanova, S. Dew, Jpn. J. Appl. Phys. 51 (2012) 06FC05 (8pp).

[31] E. A. Dobisz, S. L. Brandow, R. Bass, J. Mitterender, J. Vac. Sci. Technol. B 18 (2000) 107–111.

[32] R. Kirchner, A. Schleunitz, H. Schift, J. Micromech. Microeng. 24 (2014) 055010 (7pp).

[33] R. Kirchner, H. Schift, J. Vac. Sci. Technol. B 32 (2014) 06F701 (7pp).

[34] V. Guzenko, N. Belić, C. Sambale, A. Schleunitz, C. David, in: Proc. 37th Int. Conf. on Micro and Nano Engineering 2011, O-LITH-40.

[35] D. J. Meyer, B. P. Downey, R. Bass, D. S. Katzer, S. C. Binari, in: Proc. Int. Conf. on Comp. Semic. Manuf. Tech. 2012, 8a.1.049.


ACCEPTED MANUSCRIPT

ACCEPTED MANUSCRIPT

## Graphical Abstract

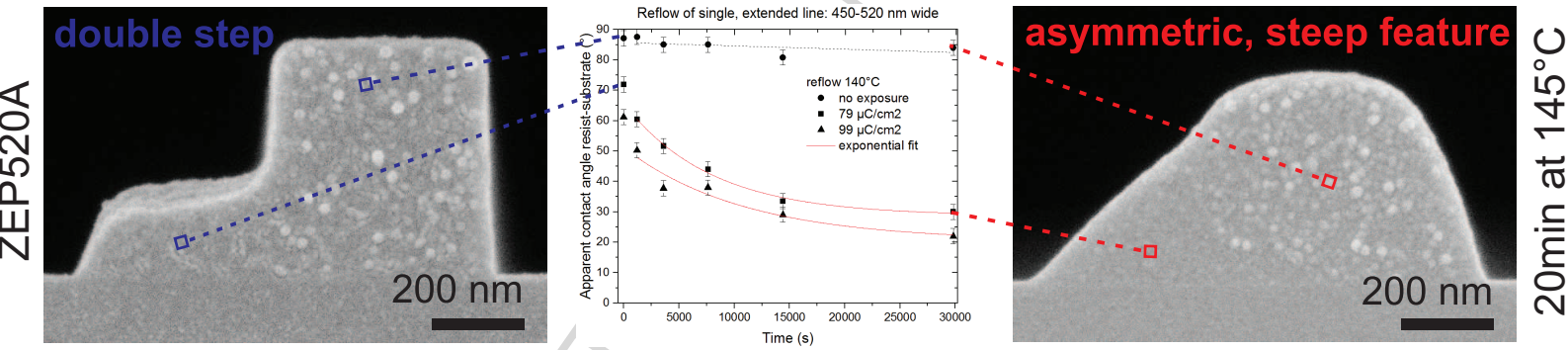

ACCEPTED MANUSCRIPT

**Highlights**

- ZEP520A is a grayscale electron beam lithography resist.
- ZEP520A supports selective thermal reflow based on selective electron exposure.
- Step-to-step sidewall angles do not depend on the resist-developer system.
- The high sensitivity of ZEP520A is its most important benefit for grayscale patterning.

ACCEPTED MANUSCRIPT